Synthesis and Solid-State NMR Studies of *P*-Vinylbenzylphosphonic Acid

Richard Frantz,[a] Jean-Olivier Durand,*[a] Francis Carré,[a] Gérard F. Lanneau,[a] Jean Le Bideau,[a] Bruno Alonso,[b] and Dominique Massiot*[b]

Abstract: *P*-Vinylbenzylphosphonic acid (**2**) was synthesized and crystallized in two phases A and B. The latter phase was easily converted into the former. Both phases were investigated by IR and solid-state ^{31}P and ^{1}H NMR spectroscopy, and X-ray crystallography. The use of recently developed NMR methods has enabled us to increase the usually poor resolution of solid-state ^{1}H spectra. This gave additional insights on the proton environments. In particular, two dimensional 2D ^{1}H-^{31}P heteronuclear correlation (HETCOR) experiments, incorporating a Lee–Golburg homonuclear decoupling scheme, allowed description of the mixture of phase A and B.

Keywords: NMR spectroscopy · phosphonic acid · structure elucidation · styrene

Introduction

The use of the phosphonic acid functionality has recently attracted much attention in a variety of different fields.[1] Elaboration of hybrid organic–inorganic materials by self-assembly of metal phosphonates precursors[1d–f] or grafting of the precursor on metal oxides have been developed.[1g–j] Phosphonic acid modified polymers have been investigated and led to polymeric resins that can be used for metal separation or metal sorption from solutions.[1a–c] In this context, structure and hydrogen bonding of phosphonic acids have an important influence on their properties. Few X-ray and solid-state ^{13}C and ^{31}P NMR studies of crystalline phosphonic acids have been reported.[2] One study involves solid-state ^{1}H CRAMPS NMR spectroscopy of carboxylic, phosphinic, and phosphonic acids, and isotropic shifts of acid protons were correlated to O···O distances.[2c] Recent developments of ^{1}H solid-state NMR spectroscopy are of great importance for the analyses of hydrogen bonding in phosphonic acids. Several new methods have been proposed for indirectly decoupling the strong $^{1}H-^{1}H$ dipolar interactions.[3–4] These methods have increased the resolution of ^{1}H spectra and allow heteronuclear correlation $^{1}H-X$ to be made through heteronuclear dipolar or scalar couplings.[4] The characterization of hybrid organic–inorganic materials can be substantially improved by this method.[5] In the course of our efforts concerning the preparation of new hybrid organic–inorganic phosphonate-based materials,[1j] we present here an improved synthesis of *P*-vinylbenzylphosphonic acid (**2**) which was first described for applications in dental research.[6] Depending on the solvent employed, it was crystallized in two phases that were carefully analyzed by X-ray crystallography and improved solid-state NMR experiments.

Results and Discussion

Phosphonic acid **2** has mainly been reported as a styrenyl polymer. Boutevin has described the monocyclohexylammonium salt[1c] of acid **2**, as the treatment of ester **1** by TMSBr then MeOH led to the anhydride (formation of P-O-P links). We first revisited the synthesis of diacid **2** from diester **1** (Scheme 1).

Nucleophilic substitution of chlorobenzylstyrene by the sodium salt of diethylphosphite gave phosphonate **1** in 94% yield. This reaction gives a higher yield than the Arbuzov

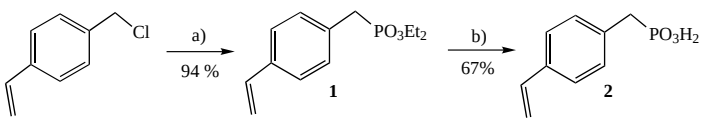

Scheme 1.

[a] Dr. J.-O. Durand, Dr. R. Frantz, Dr. F. Carré, Dr. G. F. Lanneau, Dr. J. Le Bideau
Laboratoire de Chimie Moléculaire et Organisation du Solide
UMR 5637, case 007, Université Montpellier 2
Place Eugène Bataillon
34095 Montpellier cedex 05 (France)
Fax: (+33) 0-4-67-14-38-52
E-mail: durand@univ-montp2.fr

[b] Dr. D. Massiot, Dr. B. Alonso
Centre de Recherche Matériaux Hautes Températures
UPR-CNRS 4212, 1 avenue de la recherche scientifique
45071 Orléans cedex 2(France)
Fax: (+33) 0-2-38-63-81-03
E-mail: massiot@cnrs-orleans.fr

Supporting information for this article is available on the WWW under http://www.chemeurj.org or from the author.

0947-6539/03/0903-0770 $ 20.00+.50/0

reaction, which requires higher temperature and longer reaction time with a benzylic chloride, and also formation of oligomers are observed in this case. Treatment of phosphonate **1** by TMSBr led to the silyl ester intermediate. Evaporation must be carried out with care in order to eliminate any traces of TMSBr before hydrolysis, because the formation of HBr catalyses the polymerization of styrene. Careful hydrolysis (H_2O) of the silyl intermediate led to the desired crude phosphonic acid **2**, which was then recrystallized from MeCN or from H_2O, (67% yield). When this recrystallization (performed with care due to easy polymerization of **2**) was carried out in MeCN, a single phase called A was obtained. When recrystallization was performed in water, another single phase B was obtained, but this phase easily undergoes transformation. Classical liquid-state NMR studies with ^1H, ^{13}C, and ^{31}P nuclei showed without ambiguity the presence of the same molecule for both phases. The chemical shift of the ^{31}P signal varies as a function of the solvent employed at least from $\delta = 22.6$ ([D_6]DMSO) to 28.2 ppm (CD_3CN).

The packing diagram of the monocrystal structure of diacid **2** in phase A is presented in Figure 1. Here, the diacid crystallizes in the centrosymmetric monoclinic space group

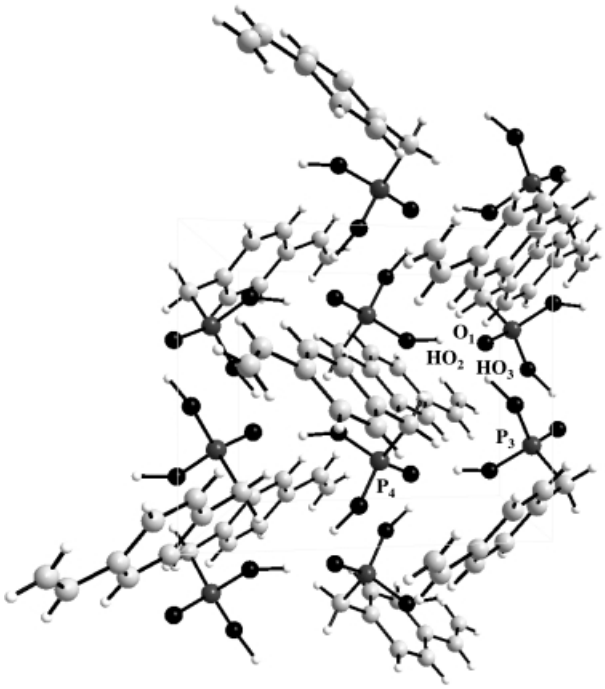

Figure 1. X-ray structure of phase A.

$P2_1/a$. Only one crystalline site for the phosphorus atom is observed. The figure, shown along the *c* axis emphasizes the connection between phosphonic acids. The P=O group is connected through two strong hydrogen bonds to two POH groups belonging to two other molecules. The lengths of these hydrogen bonds are short ($O1\cdots HO3 = 1.53$ Å, $r(O1\cdots O3) = 2.60$ Å, $O1\cdots HO2 = 1.40$ Å, $r(O1\cdots O2) = 2.55$ Å), and the angle between them is 86.67°. The hydrogen bonds between phosphonic groups form a hydrophilic layer and govern the orientation of the organic part. The distance between two adjacent layers is 13.57 Å. The aromatic groups are orientated towards the interlayer space; this results in an intercalated hydrophobic layer. The value of the dihedral angle formed by the phenyl ring and the double bond is 0.2°, which shows the coplanarity of the conjugated system in the solid state. The angle between two adjacent aromatic groups is 81° (e.g., molecules P3 and P4 which are nearly perpendicular). The related solid-state ^{31}P spectrum (Figure 2a) shows a

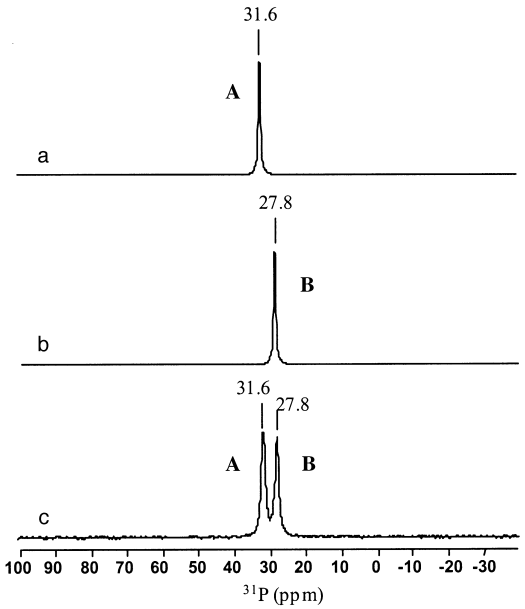

Figure 2. ^{31}P proton decoupled CP MAS spectra of diacid **2** recrystallized a) from MeCN, b) from H_2O, and c) after partial dehydration. The delay between scans was 4 s, the contact time 1.5 ms, and four scans were recorded.

narrow single peak at $\delta = 31.6$ ppm, as expected from the crystal structure of phase A, in which only one phosphorus site is involved. The IR spectrum of phase A showed strong and broad resonances at 2750 cm^{-1} and at 2320 cm^{-1}, overlapping each other, and are characteristic of intermolecular P-O-H$\cdots$O=P hydrogen bonds with phosphonic acids.[7] The ^1H NMR spectra of phase A are presented in Figure 3.

In standard conditions (Larmor frequency ν_L of 300 MHz, and magic angle spinning Rate ν_{MAS} of 11 kHz), no resolved peaks could be observed because of the intense $^1H-^1H$ homonuclear dipolar couplings (Figure 3a). With high magnetic fields and spinning rates (e.g. $\nu_L = 600$ MHz, and $\nu_{MAS} =$ 35 kHz), these couplings are strongly reduced, and a much better resolved spectrum can be obtained (Figure 3b). Simulation of this spectrum by a home-developed software[8] allowed to distinguish eight lines that can be ascribed to the different proton sites of the structure by reference to the proton chemical shifts in the liquid state (Figure 3c–d).

The IR spectrum of pure phase B (obtained just after recrystallization from H_2O, drying under air flux for 1 h and then in air for 3 h) showed resonances at 3560 and 3273 cm^{-1} characteristic of ν(OH) of H_2O in weak interaction with hydrogen bonds. The resonance of POH at 2750 cm^{-1} is much weaker than for phase A, and did not overlap with bands at 2320 cm^{-1} and at 3085–2950 cm^{-1} (ν(CH)). Thus, the hydro-

  0947-6539/03/0903-0771 $ 20.00+.50/0

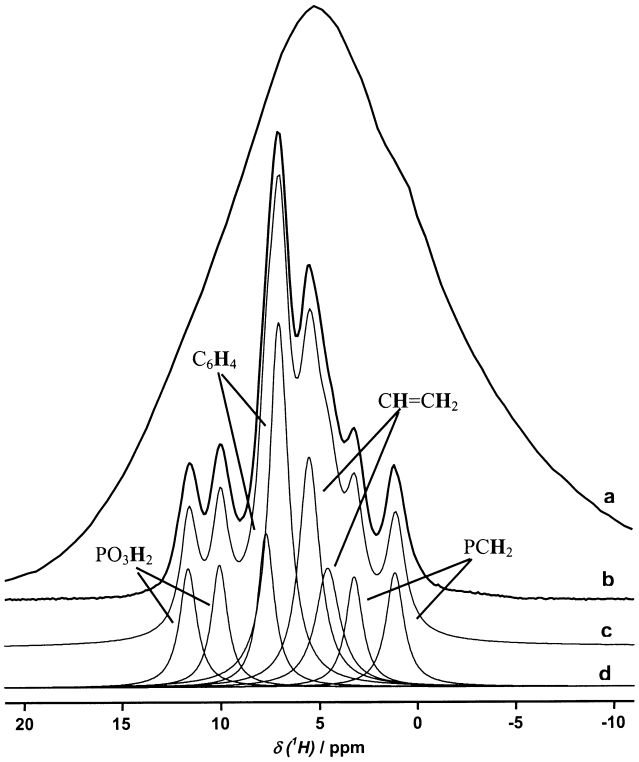

Figure 3. ^{1}H MAS single pulse spectra of phase A recorded at: a) $\nu_L =$ 300 MHz and $\nu_{MAS} = 11$ kHz; b) $\nu_L = 600$ MHz and $\nu_{MAS} = 35$ kHz. c) Simulated spectrum and d) signal decomposition used. Eight scans were recorded at intervals of 10 s.

gen-bond structure of P-O-H with P=O and OH groups in phase B is different from that of phase A. A broad resonance at 1693 cm^{-1} characteristic of a δ(OH) of H_2O appeared. Phase B contains water molecules that interact with phosphonic groups. The solid-state ^{31}P NMR spectrum showed a single signal at $\delta = 27.8$ ppm (Figure 2b) with a width at half maximum of 2 ppm, indicating a second well-organized system. The X-ray diffraction (XRD) pattern (Figure 4) of

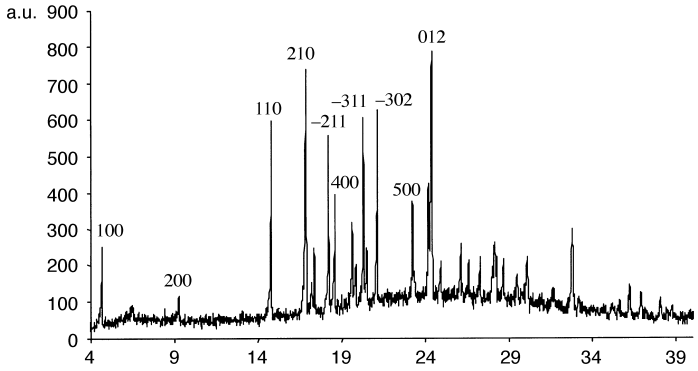

Figure 4. X-ray powder diffraction diagram of phase B.

pure phase B allowed us to determine the cell parameters of the crystal structure after indexing the diagram by calculation. Phase B crystallizes in a monoclinic system, and the distance between two layers is increased to 19 Å. The structure of layered Zn phosphonates with intercalated water molecules have been described by Bujoli.[1e–f] Water molecules were interacted weakly through hydrogen bonds with phosphonate oxygen atoms, allowing easy dehydration of the crystal at 30–40 °C. In our case, lattice water molecules increases the interlayer distance of phase B to 19 Å. These molecules are bonded to phosphonic groups by weak hydrogen bonds (IR) as pure phase B is very easy to dehydrate. When crystals of phase B were dried under vacuum at room temperature for 2 h, the ^{31}P peak at $\delta = 27.8$ ppm disappeared almost completely and signal at $\delta = 31.6$ ppm appeared. When solid-state ^{31}P NMR spectra of phase B were recorded at increasing spinning rates (ν_{MAS} from 15 to 35 kHz), we also observed the disappearance of the signal at $\delta = 27.8$ ppm probably due to some heating and centrifugation. Thus, it was not possible to obtain a well resolved ^{1}H spectrum of phase B by using high spinning rates.

We then studied phase B after partial dehydration of the crystals. Solid-state ^{31}P NMR spectrum showed two signals at $\delta = 27.8$ and 31.6 ppm (Figure 2c) associated with two non-equivalent phosphorus sites. The IR spectrum showed disappearance of resonances at 3560 and 3273 cm^{-1} and strengthening of resonance at 2750 cm^{-1}. The XRD pattern (Figure 5) contained diffraction peaks related to phase A and to phase B (indexation of phase A is shown).

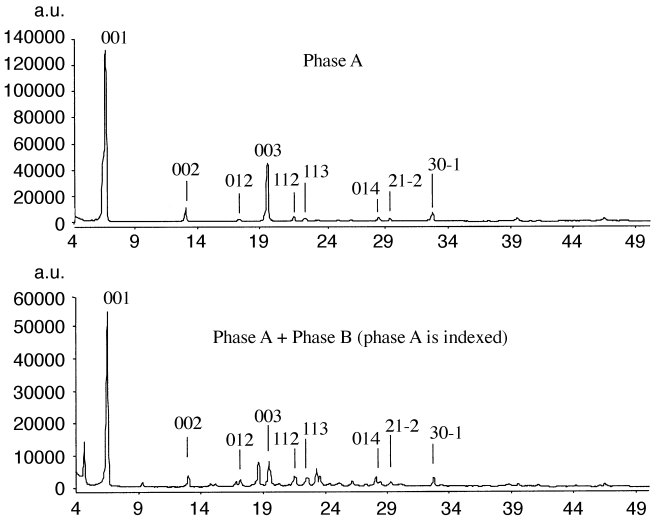

Figure 5. X-ray powder diffraction diagrams of diacid **2** recrystallized a) in MeCN and b) in H_2O after partial dehydration.

These results are in agreement with data reported by Merwin.[2a] Dimethylaminomethanediphosphonic acid and its monohydrate were characterized by the same techniques and major changes were observed in the XRD and solid-state ^{31}P NMR data, indicating that the diacid and the monohydrate were crystallized in two different systems with quite different unit cells. Approximately 5–10% of the anhydrous phase was present in the hydrate. In our case, phase B dehydrates to give phase A, and the coexistence of the two phases was therefore analyzed. To study ^{1}H NMR signature of both phases A and B in the partially dehydrated crystals, a possibility is to perform a two-dimensional heteronuclear correlation experiment (HETCOR) between the ^{1}H and ^{31}P nuclei[9] at a spinning rate of $\nu_{MAS} = 15$ KHz. The intensity of the cross-peaks

0947-6539/03/0903-0772 $ 20.00+.50/0 *Chem. Eur. J.* **2003**, *9*, No. 3

between ^{1}H and ^{31}P signals were monitored by the contact time τ_c during cross-polarization $^1H \rightarrow {}^{31}P$. At short τ_c, cross-peaks between ^{1}H and ^{31}P signals will depend on the strength of direct ^{1}H–^{31}P heteronuclear dipolar couplings. Typically, H–P distances explored are in the range 1–5 Å. At longer τ_c, the ^{1}H spin diffusion process involving ^{1}H–^{1}H homonuclear dipolar couplings becomes significant. Other cross-peaks could thus appear between signals of more distant ^{1}H and ^{31}P nuclei (up to several nanometers). Therefore, a qualitative picture on the spatial proximity of the different sites could emerge. However, under standard conditions, ^{1}H signals would not be resolved (see for example Figure 3a). This difficulty can be overcome by introducing a Lee–Golburg decoupling scheme[10] during the evolution time of protons t_1 (the effective magnetic field is maintained at the magic angle with respect to the static field which averages out ^{1}H–^{1}H homonuclear dipolar couplings in a first-order approximation). This Lee–Golburg decoupling scheme is achieved by implementing an off-resonance[11] or a phase-modulated radio frequency irradiation.[3a] Figure 6 represents two of the resulting spectra from two-dimensional ^{1}H–^{31}P experiments on mixed phase A and B. Phases A and B selected by their ^{31}P resonances have different ^{1}H signatures. At short contact time $\tau_c = 0.1$ ms, different cross-peaks between CH_2 and PO_3H_2 ^{1}H signals and PO_3H_2 ^{31}P signals are observed. Indeed, H–P distances for these groups are short : 2.28 Å (phase A Figure 1).

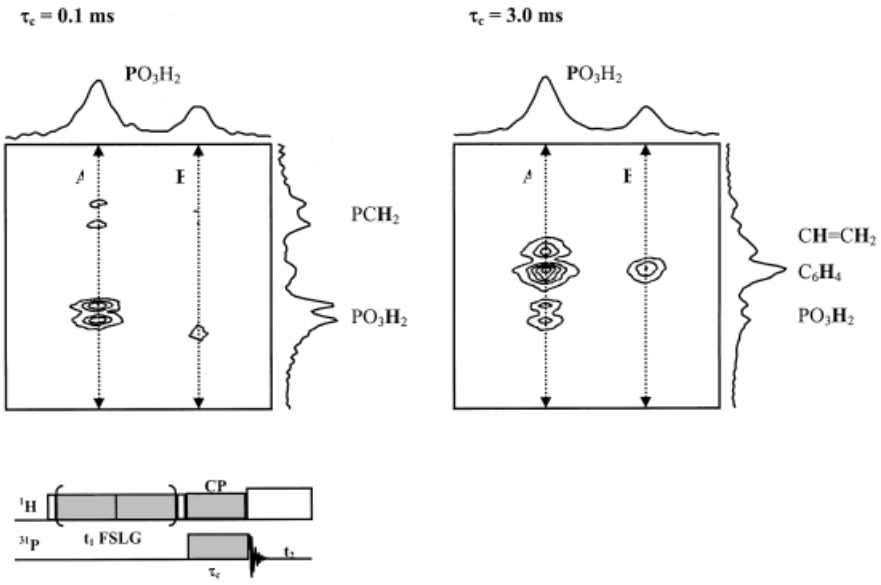

Figure 6. ^{1}H–^{31}P two-dimensional heteronuclear correlation by means of frequency-shifted Lee–Golburg ^{1}H decoupling and $^1H \rightarrow {}^{31}P$ cross-polarization[3a] during variable contact times τ_c. A simplified scheme of the radio-frequency pulse sequence is also shown. The delay between scans was fixed at 1 s; 8 dummy scans were employed and 16 scans per slice were recorded.

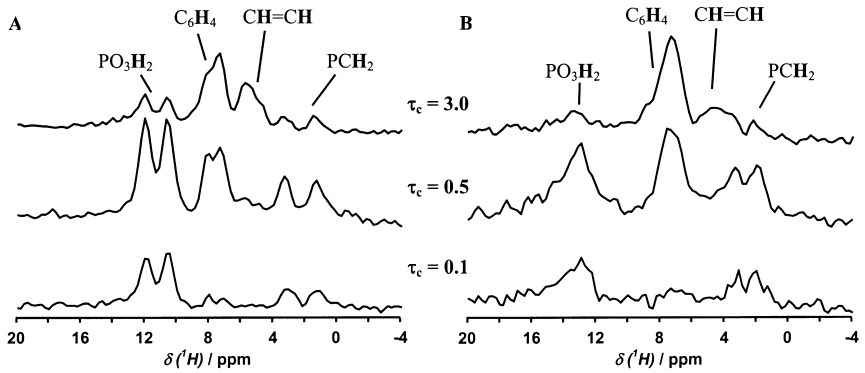

Figure 7. ^{1}H spectra obtained from ^{1}H–^{31}P two-dimensional experiments (described in the text and in Figure 5) at $\delta(^{31}P) = 32$ ppm (A) and $\delta(^{31}P) = 28$ ppm (B). Contact times τ_c employed during cross-polarization are detailed for the three sets of spectra. Spectrum intensities are comparable within each phase A or B.

When increasing τ_c, cross-peaks between aromatic then vinylic ^{1}H signals and PO_3H_2 ^{31}P signals are detected. The distances between aromatic protons and phosphorus are in the range of 3.38–5.82 Å, and those between vinylic protons and phosphorus are the largest, in the range of 5.00–6.10 Å. The cross-peaks related to phases A and B were differentiated by considering vertical sections at their respective ^{31}P resonances (Figure 6). The resulting ^{1}H spectra are presented in Figure 7 for three contact times τ_c, and for the two phases.

Signals of phase A are in good agreement with those obtained at high magnetic field and high spinning rate (Figure 3). In the case of phase B, we observe similar signals but at slightly different chemical shifts; this again evidences the existence of two distinct phases. The most striking difference is related to PO_3H_2 ^{1}H signals. Two ^{1}H signals are observed for phase A instead of a single but wider signal for phase B (Table 1). The related chemical shifts depend on the strength of the hydrogen bonds.[12]

In the case of phase A, one terminal P=O group makes two different hydrogen bonds with two hydroxyl groups (vide

Table 1. ^{31}P and ^{1}H chemical shifts of phosphonic groups in *d*-DMSO solution and in phases A and B, with related hydrogen-bond lengths.

	δ ^{31}P [ppm]	δ ^{1}H [ppm]	H-bond length [Å] ref. [2c]
$[D_6]$DMSO	22.2	8.8	
Phase A	31.6	10.1[a]–10.5[b]	$2.62 < r(O\cdots O) < 2.67$
	31.6	11.7[a]–11.5[b]	$2.55 < r(O\cdots O) < 2.59$
Phase B	27.8	12.5[b]	average $r(O\cdots O) = 2.53$

[a] Spectrum simulated in Figure 4 (precision 0.1 ppm). [b] Spectra in Figure 6 (precision 0.5 ppm).

  0947-6539/03/0903-0773 $ 20.00+.50/0

supra) leaving to two different ^{1}H signals. Following Harris' work[2c] in which the isotropic shielding of acidic protons were correlated to the oxygen – oxygen bond distance for hydrogen bonds of phosphonic acids, the shift of 10.5($\pm$0.5) ppm for H3 corresponds to $2.62 < r(O1\cdots O3) < 2.67$ Å. The shift of 12($\pm$0.5) ppm for H2 corresponds to $2.55 < r(O1\cdots O2) < 2.59$ Å. Crystallographic measurements gave $r(O1\cdots O3) = 2.60$ Å and $r(O1\cdots O2) = 2.55$ Å. Thus, correlation results are in agreement with crystallographic measurements with less than 5% error. The single broadened PO_3H_2 signal for phase B indicated different contributions, with a higher mobility of the phosphonic proton environment. If this bond consists on one P=O group linked to one hydroxyl group, or one hydroxyl group linked to another one, its length can be calculated following Harris' correlation.[2c]. Considering a chemical shift of $\delta = 12.5$ ppm, we obtained an average distance $r(O\cdots O) = 2.53$ Å, which is close to the O$\cdots$O distances calculated in phase A.

Conclusion

We have revisited the synthesis of styrenyl phosphonic acid **2**. Its crystals were studied by X-ray crystalography and NMR experiments; this allowed us to differentiate two crystalline phases, one anhydrous phase A and one hydrated phase B, with different hydrogen bonding features. Description of the proton environments in these two phases was performed by using recent high-resolution ^{1}H NMR experiments. Information brought by these studies will be useful for the modification of surface metal oxides by reaction with acid **2** in which one, two, or three P-O-metal bonds are involved.

Experimental Section

All reactions were carried out under an argon atmosphere. Solvents were dried by standard methods and were distilled prior to use. ^{1}H, ^{13}C, and ^{31}P NMR liquid-state spectra were obtained on a Bruker AC200 spectrometer. IR spectra were recorded on a Perkin – Elmer 1600 FT spectrometer. Mass spectra were recorded on a Jeol JMS-DX300 instrument using FAB$^+$ mode with a glycerol-thioglycerol (GT) matrix. Powder diffraction diagrams were registered on a X'Pert Philips diffactometer with a copper anticathode (Kα1). Simulation of powders diffraction diagrams were performed with Poudrix software (J. Langier and B. Bochu) and indexations were performed with TREOR program. Single-crystal X-ray structure was performed with an Enraf-Nonius CAD4 (four circle) diffractometer.

All solid-state NMR spectra were recorded on a Bruker DSX300 spectrometer (7 T), except the ^{1}H high magnetic field spectra, which were recorded at 14 T. Spectra were referenced relative to TMS and H_3PO_4 at 0 ppm for ^{1}H and ^{31}P, respectively. Radio-frequency fields between 50 to 60 kHz were employed. A ramp for polarization transfer[10] was used in cross polarization (CP) and FSLG-CP experiments to obtain a broad Hartmann – Hahn match condition and improve signal-to-noise ratio.

Diethyl *P*-vinylbenzylphosphonate: NaH (50% in grease, 6.52 g, 0.163 mol) was suspended in THF (170 mL) at 0 °C. Diethylphosphite (25.3 mL, 0.196 mol) was added drop wise. The mixture was allowed to come to RT, then transferred by cannula to a solution of 1-chloromethyl-4-vinylbenzene (25g, 0.163 mol) and NaI (2.44 g, 16.3 mmol) in THF (170 mL) at 0 °C. The solution turned from pale yellow to orange. The mixture was stirred overnight. Salts were precipitated by the addition of AcOEt, and the mixture was filtered through celite. Volatiles were removed, and the residue was purified by flash chromatography (eluant : AcOEt). The product was isolated as a pale yellow oil (39 g, 94%). ^{1}H NMR ($CDCl_3$): $\delta = 7.33$ (d, $^3J = 8.2$ Hz, 2H), 7.21 (dd, $^3J = 8.2$ Hz, $^3J = 2.2$ Hz, 2H), 6.66 (dd, $^3J = 16.7$ Hz, $^3J = 10.9$ Hz, 1H), 5.7 (d, $^3J = 16.7$ Hz, 1H), 5.2 (d, $^3J = 10.9$ Hz, 1H), 4.22-3.98 (m, 4H), 3.11 (d, $^2J = 21.8$ Hz, 2H), 1.26 ppm (t, $^3J = 7.1$ Hz, 6H); ^{13}C NMR ($CDCl_3$): $\delta = 136.74$ (dd, $^6J = 2.1$ Hz, 1C), 136.52 (d, $^5J = 3.9$ Hz, 1C), 131.51 (d, $^2J = 9.3$ Hz, 1H), 130.24 (dd, $^3J = 6.7$ Hz, 2C), 126.65 (dd, $^4J = 3.2$ Hz, 2C), 113.95 (td, $^7J = 1.5$ Hz, 1C), 62.38 (td, $^2J = 6.7$ Hz, 2C), 33.82 (td, $^1J = 173.1$ Hz, 1C), 16.69 pp, (qd, $^3J = 5.9$ Hz, 2C); ^{31}P NMR ($CDCl_3$): $\delta = 27.4$ ppm; IR: $\tilde{\nu} = 3100, 2981, 2840, 1630, 1513, 1408, 1248, 1163, 1028, 980 – 860$ cm^{-1}.

***P*-Vinylbenzylphosphonic acid**: Diethylparavinylbenzylphosphonate (10 g, 39.4 mmol) was dissolved in CH_2Cl_2 (50 mL). TMSBr (18.08 g, 0.19 mol) was added, and the reaction was stirred overnight. The mixture was concentrated in vacuo and the oily residue was hydrolyzed with H_2O (11.7 mL, 0.65 mol). The white precipitate was filtered and recrystallized from H_2O or CH_3CN and dried in air. The product was isolated as white needles (5.2 g, 67%). M.p. 164 – 167 °C; ^{1}H NMR ([D$_6$]DMSO): $\delta = 8.79$ (s, 2H), 7.39 (d, $^3J = 8$ Hz, 2H), 7.23 (d, $^3J = 8$ Hz, 2H), 6.71 (dd, $^3J = 10.9$ Hz, $^3J = 17.7$ Hz, 1H), 5.79 (d, $^3J = 17.7$ Hz, 1H), 5.22 (d, $^3J = 10.9$ Hz, 1H), 2.96 ppm (d, $^2J = 21.6$ Hz, 2H); ^{13}C NMR ([D$_6$]DMSO): $\delta = 137.4$ (d, 1C), 135.8 (dd, $^4J = 3.7$ Hz, 2C), 135. 0 (d, $^2J = 9.0$ Hz, 1C), 130.8 (dd, $^3J = 6.3$ Hz, 2C), 126.6 (d, $^5J = 3$ Hz, 1C), 114.4 (t, 1C), 36.1 ppm (td, $^1J = 131.7$ Hz, 1C); ^{31}P NMR ([D$_6$]DMSO): $\delta = 22.2$ ppm; HR MAS (FAB+, GT): calcd: 199.0589; found: 199.0524.

Phase A: IR (KBr): 3558, 2750, 2317, , 1629, 1511, 1407, 1267, 1233, 1098, 998, 910, 846, 803 cm^{-1}.

Phase B: IR (KBr): 3560, 3273, 3086, 3043, 3006, 2952, 2722, 2340, 1693, 1511, 1407, 1261, 1224, 1145, 1098, 1010, 953, 910, 846, 803 cm^{-1}.

X-ray powder calculation for phase B (TREOR): $a = 9.065(2)$, $b = 6.313(1)$, $c = 19.993(3)$ Å; $\beta = 107.25(1)^\circ$; $M(20) = 49$, $F(20) = 107.(0.003903, 48)$.

CCDC-200070 contains the supplementary crystallographic data for this paper. These data can be obtained free of charge via www.ccdc.cam.ac.uk/conts/retrieving.html (or from the Cambridge Crystallographic Data Centre, 12 Union Road, Cambridge CB2 1EZ, UK; fax: (+44) 1223-336033; or deposit@ccdc.cam.uk). Data collection parameters are available as Supporting Information.

Acknowledgement

We thank Professor G. Bodenhausen (ENS, Paris) for the access to the Bruker 600 spectrometer. We thank the referees for important adivce. We acknowledge financial support from CNRS, Région Centre and European Community contracts HPRI-CT-1999-00042 and HPMT-CT-2000-00169.

[1] a) A. M. El-Naggar, A. S. Emara, S. G. Abdalla, *J. Appl. Polym. Sci.* **1997**, *65*, 1091; b) S. D. Alexandratos, M. E. Bates, *Macromolecules* **1988**, *21*, 2905; c) B. Boutevin, H. Bachar, J. P. Parisi, B. Améduri, *Eur. Polym. J.* **1996**, *32*, 159; d) G. Alberti, in *Comprehensive Supramolecular Chemistry, Vol. 7* (Ed.: J.-M. Lehn, J. L. Atwood, J. E. D. Davies, D. D. MacNinol, F. Vögtle, Pergamon, Oxford, **1996**, pp. 151 – 187; e) F. Fredoueil, V. Penicaud, M. Bujoli-Doeuff, B. Bujoli, *Inorg. Chem.* **1997**, *36*, 4702; f) F. Fredoueil, M. Evain, M. Bujoli-Doeuff, B. Bujoli, *Eur. J. Inorg. Chem.* **1999**, 1077; g) P. Bonhôte, J. E. Moser, R. Humphry-Backer, N. Vlachopoulos, S. M. Zakeeruddin, L. Walder, M. Grätzel, *J. Am. Chem. Soc.* **1999**, *121*, 1324; h) A. G. Neff, N. M. Helfrich, M. C. Clifton, C. J. Page, *Chem. Mater.* **2000**, *12*, 2363; i) C. Maillet, P. Janvier, M. Pipelier, T. Praveen, Y. Andres, B. Bujoli, *Chem. Mater.* **2001**, *13*, 2879; j) R. Frantz, J. O. Durand, G. F. Lanneau, J. C. Jumas, O.-J. Fourcade, M. Cretin, M. Persin, *Eur. J. Inorg. Chem.* **2002**, 1088.

[2] a) L. H. Merwin, W. A. Dollase , G. Hägele, H. Blum , *Phosphorus, Sulfur, Silicon* **1991**, *56*, 117; b) R. K. Harris, L. H. Merwin, G. Hägele, *J. Chem. Soc. Faraday Trans. 1* **1989**, *85*, 1409; c) R. K. Harris, P. Jackson, L. H. Merwin, B. J. Say, G. Hägele, *J. Chem. Soc. Faraday Trans. 1* **1988**, *84*, 3649; d) R. K. Harris, L. H. Merwin, G. Hägele, Magn. *Res. Chem.* **1989**, *27*, 470; e) G. Ohms, K. Krüger, A. Rabis, V. Kaiser, *Phosphorus Sulfur Silicon Relat. Elem.* **1996**, *114*, 75.

[3] a) E. Vinogradov, P. K. Madhu, S. Vega, *Chem. Phys. Lett.* **1999**, *314*, 443; b) D. Sakellariou, A. Lesage, P. Hodgkinson, L. Emsley, *Chem.*

  0947-6539/03/0903-0774 $ 20.00+.50/0 *Chem. Eur. J.* **2003**, *9*, No. 3

Phys. Lett. **2000**, *319*, 253; c) A. Lesage, L. Duma, D. Sakellariou, L. Emsley, *J. Am. Chem. Soc*. **2001**, *123*, 5747; d) P. K. Madhu, X. Zhao, M. H. Levitt, *Chem. Phys. Lett*. **2001**, *346*, 142.

[4] a) B. J. van Rossum, H. Forster, J. H. de Groot, *J. Magn. Reson*. **1997**, *124*, 516; b) A. Lesage, D. Sakalleriou, S. Steuernagel, L. Emsley, *J. Am. Chem. Soc*. **1998**, *120*, 13194.

[5] a) V. Ladizhansky, G. Hodes, S. Vega, *J. Phys. Chem. B* **2000**, *104*, 1939; b) D. Massiot, B. Alonso, F. Fayon, F. Fredoueil, B. Bujoli *Solid State Sci.* **2001**, *3*, 11.

[6] M. Anbar, G. A. St. John, A. C. Scott, *J. Dent. Res.* **1974**, 867.

[7] R.R Holmes, R. O. Day, Y. Yoshida, J. M. Holmes, *J. Am. Chem. Soc.* **1992**, *114*, 1771.

[8] D. Massiot, F. Fayon, M. Capron, I. King, S. Le Calvé, B. Alonso, J. O. Durand, B. Bujoli, Z. Gan, G. Hoatson, *Magn. Reson. Chem.* **2002**, *40*, 70.

[9] After excitation ^{1}H nuclei evolve during an incremented time t_1. Cross-polarization (CP) is used afterwards to transfer ^{1}H polarization to ^{31}P nuclei during a contact time τ_c. Finally, ^{31}P signals are acquired during t_2. A double Fourrier transform allows us then to obtain a two-dimensional spectrum with ^{1}H and ^{31}P signals along the $F1$ (vertical) and $F2$ (horizontal) dimensions, respectively.

[10] M. Lee, W. I. Golburg, *Phys Rev. A* **1965**, *140*, 1261.

[11] A. Bielecki, A. C. Kolbert, M. H. Levitt, *Chem. Phys. Lett.* **1989**, *155*, 341.

[12] E. Brunner, U. Sternberg, *Prog. Nucl. Magn. Reson. Spectrosc*. **1998**, *32*, 21.

[13] G. Metz, X. Wu, S. O. Smith, *J. Magn. Reson. A* **1994**, *110*, 219.

Received: March 13, 2002
Revised: October 7, 2002 [F3947]

  0947-6539/03/0903-0775 $ 20.00+.50/0